Ecological Informatics 93 (2026) 103540

Contents lists available at ScienceDirect

Ecological Informatics

journal homepage: www.elsevier.com/locate/ecolinf

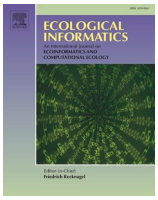

Whiteboard photography: A field method with automated image processing to measure vertical vegetation features for ecological research in open habitats

Gergő Oláh [a,b,*], Mátyás Budai [c,d], Edvárd Mizsei [d,e,f], Miklós Bán [a]

[a] HUN_REN-DE Behavioural Ecology Research Group, Department of Evolutionary Zoology and Human Biology, University of Debrecen, Debrecen, Hungary
[b] Doctoral School of Informatics, University of Debrecen, Debrecen, Hungary
[c] Juhász-Nagy Pál Doctoral School, University of Debrecem, Hungary
[d] Centre for Metagenomics, University of Debrecen, Debrecen, Hungary
[e] Kiskunság National Park Directorate, Kecskemét, Hungary
[f] Conservation Ecology Research Group, Institute of AquaticEcology, HUN-REN Centre for Ecological Research, Debrecen, Hungary

ARTICLE INFO

Keywords:
Vegetation structure
Automated image processing
Object detection
Habitat modeling
Lizard density
Open habitats
YOLO

ABSTRACT

Accurate measurement of vertical vegetation structure is essential for modeling habitat variation and species interactions. The study's objective to present an improved *whiteboard photography* method combined with a semi-automated image processing pipeline to standardize vegetation measurements in open habitats. The workflow includes whiteboard localization using a neural network for real-time object detection; geometric correction based on reference points; pixel-level vegetation classification; and calculation of structural metrics such as leaf area (LA: total leaf surface), maximum height of vegetation (MHV: tallest point), height of closed vegetation (HCV: lowest continuous cover), and foliage height diversity (FHD: height variation). All steps are integrated into a web interface that enables both user-controlled and fully automated image processing within seconds per image.

Geometric transformation accuracy and noise sensitivity were evaluated using 120 calibration images. Object-detection precision was high ($mAP_{50} \approx 0.995$, where mAP_{50} represents mean average precision at 50 % intersection-over-union). Over 92.9 % of cases exhibited geometric error $\leq$ 5 cm, regardless of whiteboard or image quality. Results indicated that renewing the board and using higher-resolution images improved measurement consistency, while moderate occlusion had minimal impact on transformation accuracy.

The method was applied to 99 Hungarian grassland plots to model Balkan Wall Lizard density using N-mixture models. Lizard density increased with greater MHV and HCV but decreased with higher LA after accounting for temperature-dependent detectability.

This low-cost, non-destructive, and replicable approach provides a reliable tool for measuring vertical vegetation structure and supports ecological monitoring and habitat modeling in open landscapes.

1. Introduction

Environmental heterogeneity creates a dynamic array of habitats, influencing the availability of resources such as food, shelter, and breeding sites for different species (Stein et al., 2014; Uetz, 1991). In terrestrial ecosystems, vegetation structure—encompassing features such as plant height, density, and species composition—forms a significant component of environmental heterogeneity (Kreft and Jetz, 2007; Loke et al., 2015). This structural complexity shapes species' distribution and habitat selection (Stein and Kreft, 2015; Tews et al., 2004). Habitat selection refers to the process by which animals choose specific areas within their broader environment based on the suitability of these areas for meeting their biological needs, such as feeding, sheltering, breeding, and escaping predators (Cody, 1981).

Vegetation structure directly influences the habitat selection process, as it determines the availability and quality of potential habitats

* Corresponding author at: HUN_REN-DE Behavioural Ecology Research Group, Department of Evolutionary Zoology and Human Biology, University of Debrecen, Debrecen, Hungary.
E-mail address: olah.gergo@science.unideb.hu (G. Oláh).

https://doi.org/10.1016/j.ecoinf.2025.103540
Received 7 June 2025; Received in revised form 28 November 2025; Accepted 28 November 2025
Available online 2 December 2025

(Novotny et al., 2006; Tews et al., 2004). Species often exhibit preferences for particular vegetation types or structures, as these structures may offer the most suitable conditions for survival and reproduction (Lawton, 1983; McCoy and Bell, 1991). Furthermore, the complexity and diversity of vegetation may increase the number of microhabitats available, thus enhancing the suitability of an area for a wider range of species. This is particularly evident in the case of arthropods, small mammals, reptiles, and other taxa whose distributions are strongly influenced by the availability of such microhabitats (Garden et al., 2007; Lengyel et al., 2016).

The role of vegetation structure extends beyond providing resources for species; it also plays a pivotal role in determining the detectability of animals, which is crucial for estimating their population sizes and distribution. For many species, especially those that are cryptic or small, detecting individuals in dense vegetation can be particularly challenging. The structural complexity of vegetation influences the effectiveness of traditional monitoring methods, such as direct visual surveys or capture-recapture studies, making it essential to account for these factors when assessing population and habitat use. Therefore, understanding how variations in vegetation structure influence species detectability, habitat selection and preferences critical for improving ecological surveys and conservation efforts (Boulinier et al., 1998).

Several methods have been developed to quantify vegetation structure, each offering different advantages and limitations. Traditional biomass collection involves cutting and weighing vegetation within sample areas, providing precise measurements of plant material. However, this approach is labour-intensive and destructive to the habitat, making it impractical for large-scale or repeated studies (Vermeire and Gillen, 2001). A cheaper and less invasive method is the Visual Obstruction Readings (VOR) method (Benkobi et al., 2000; Robel et al., 1970), which estimates vegetation height by measuring how much vegetation obstructs a vertical rod placed in the field. However, VOR does not provide information on other important aspects, such as leaf area or the diversity of vegetation heights. Additionally it's influenced by operator skill and can be time-consuming when multiple readings are needed.

Quickly calculating multiple parameters in parallel without observer bias is more convenient for machines than for humans. The most accessible way to feed information about vegetation structure to the computer is through images, which gave rise to powerful photographic tools for vegetation analysis in recent years (Easlon and Bloom, 2014; Zehm et al., 2003). These methods are non-destructive and efficient, and allow for the collection of data with minimal disturbance to the environment. Zehm et al. (2003) highlighted the benefits of photographic techniques, noting their ability to capture a broad range of structural parameters, such as canopy height, leaf area, and vertical stratification. Despite these advantages, these methods can still be limited by the time required to capture high-quality images, especially in dense vegetation, and by the need for specialised software for data analysis which is often outdated hindering the general usage of such methods.

To address the shortcomings of former methods, Mizsei et al., 2024 proposed a photographic method (so called whiteboard method), which uses a fixed sized whiteboard (100 cm height x 25 cm width) placed in the field to capture vegetation structure in grasslands. This method is quick, easy to use (even alone), and minimizes disturbance to the vegetation while providing detailed measurements of parameters like leaf area (LA), maximum height of vegetation (MHV), height of the closed vegetation (HCV), and foliage height diversity (FHD). To adapt the method, all one needs is simple office supplies, a mobile phone and a computer. The main limitation of this method arises during the image processing step, where the whiteboard must be cut out from the image before the pixel analysis, which is done manually. This manual cropping is time-consuming and prone to error, since finding the edges and the bottom of the whiteboard is nearly impossible in dense vegetation. Additionally, the pixel classification on the gray-scaled images is based on a single hard-coded threshold value. This rigidness makes the analysis sensitive to changing light conditions, especially when there are differences between the different parts of the board.

The primary aim of this study is to improve the whiteboard method for measuring vegetation structural heterogeneity by automating and refining the image processing workflow (Fig. 1). By integrating machine learning-based object detection and adaptive thresholding techniques, we aim to increase the efficiency and accuracy of the method, eliminating the need for manual cropping and improving pixel classification under varying lighting conditions. Additionally, we developed a user-friendly web application to facilitate the widespread use of the method in ecological studies. To validate the effectiveness of the enhanced method, we present a case study as an example for applications by examining the abundance of the Balkan Wall Lizard, a grassland specialist reptile. This case study will provide insights into how vegetation structural parameters affect the lizard's density and contribute to understanding the practical applications of the method in real-world ecological research.

2. Materials and methods

2.1. Description of the whiteboard

We used a rigid plastic whiteboard measures 105 × 35 cm (height x width) which is slightly modified compared to the one (100 × 25 cm) used in Mizsei et al., 2024 study. On the upper part of the board, at specified distances, we painted 3 different-coloured reference squares measuring 5 × 5 cm each (red, purple, blue). On the bottom of the board, we drew lines every 1 cm on each side (Fig. 2). Additionally, to avoid distortions, a batten was fixed to the back of the board in the middle to prevent the board from warping. We drove a nail into the bottom of the batten, allowing it to be easily inserted into the ground. To support consistency we attached a string to the nail, which can be used to measure distances - although the method is not severely influenced by distance, since most of the calculation are based on the relative size of the reference squares.

2.2. Taking photo on the field

Carefully place the whiteboard in the vegetation on its shorter edge, without trampling the vegetation between the whiteboard and the camera. Take a photo from approximately 0,5–1 height and 2–4 m distance. The whiteboard should be kept standing as straight as possible, and avoiding physical distortion (such as twisting, deflection). Repeat this procedure on each sampling plot.

2.3. Localization and perspective transformation

To localize the whiteboard in the images, we used YOLOv8 (Jocher et al., 2023). The images used for training the model were annotated using the CVAT (Computer Vision Annotation Tool, CVAT.Ai Corporation, 2023) software. We annotated the top third of the board on each image, by manually drawing the bounding boxes. We used custom image set taken from a distance of 2 m (measured from the bottom of the board) and a height of 80 cm and split them in three groups: 293 images for training, 36 images for validation, and 37 for testing the model. During the training process, we utilized a single GPU (NVIDIA GeForce RTX 3090), the 'nano' pre-trained (on COCO dataset, Lin et al., 2014) model, and the default training parameters. We evaluated the performance of our model using the default evaluation parameters, which resulted in 3 metrics, namely precision (indicating how many detections were correct, true positive detections divided by all detections), recall (indicating the proportion of possible objects detected, true positive detection divided by all possible detection) and mean average precision (mAP at intersection over union rate of 0.50, the area under the precision recall curve Fig. S1). After running the detection, we cropped out the image parts inside the bounding box, which contains the top of the

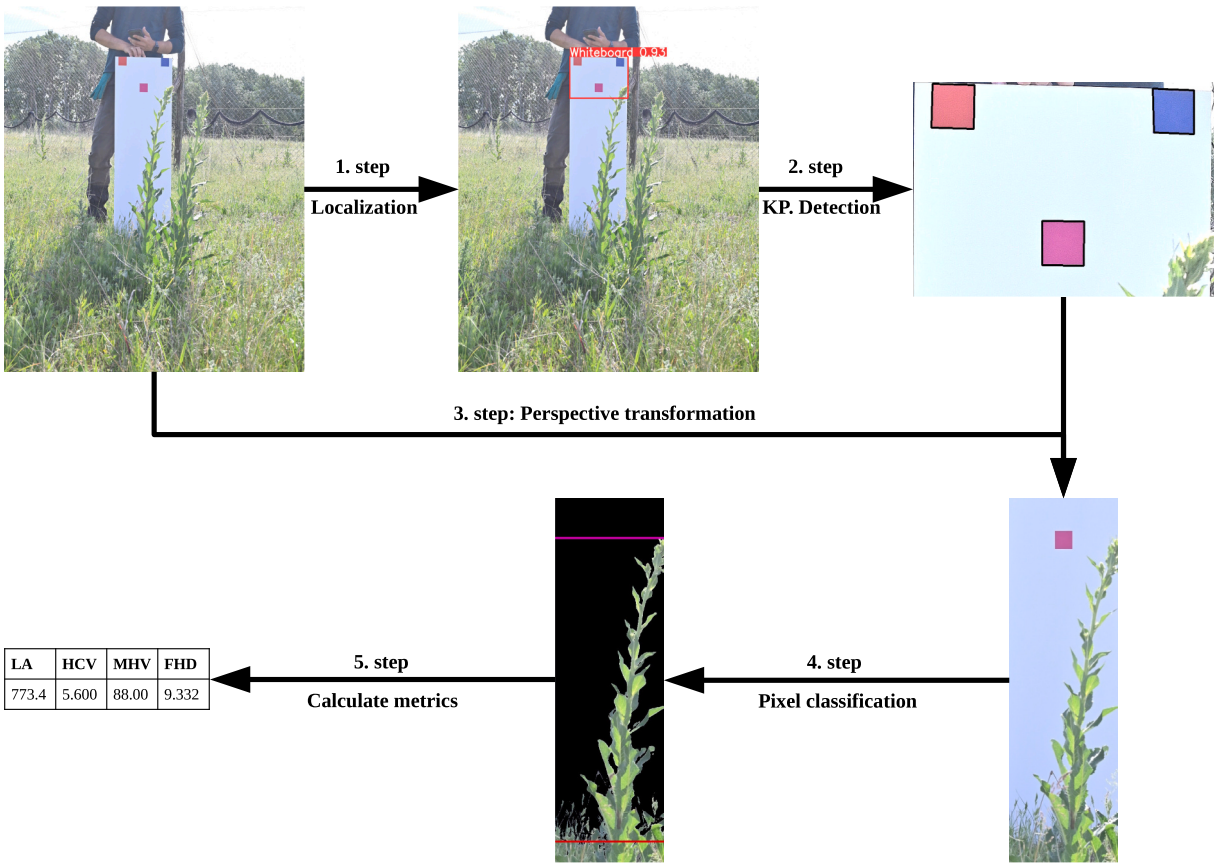

Fig. 1. Automated image processing workflow: 1. Step: Localizing the whiteboard on our original image using our YOLOV8n object detector. 2. Step: Using the sharpened "box image" (image part cut out based on bounding box coordinates) we detect the keypoint coordinates by processing the output of the Shi-Thomasi corner detector. 3. Step: Perspective transformation on the original image using the keypoint coordinates, which yields the orthophoto of the whiteboard. 4. Step: Binary classification (whiteboard or vegetation) of each pixel, based on RGB colour codes and coordinates. Based on these we can calculate (5. Step) the different structural metrics like maximum height of vegetation (MHV, illustrated with the purple vertical line), height of closed vegetation (HCV, illustrated with the red vertical line), leaf area (LA), and foliage height diversity (FHD). (For interpretation of the references to colour in this figure legend, the reader is referred to the web version of this article.)

whiteboard, resulting – in what we call – a "box image" (Fig. 1).

The projection of a three-dimensional object into a plane (including the process of taking a photograph) involves certain distortions that can never be completely avoided. Therefore, before analyzing a photograph, it is necessary to reconstruct it into a geometrically correct image (orthophoto). For this task, we used the tools provided by the OpenCV (Bradski, 2000) image processing library. The logic behind the process is that if we know the positions of an object's key points in two different images taken from different perspectives, as well as the difference between the two viewpoints, we can transform one image into the perspective of the other. In our case, we take only one photo and the process can be interpreted as follows: we can calculate the positions of certain key points on an ideal board image (frontal, non-tilted) and we detect the same key points on the board photo (possibly skewed, tilted), then through a perspective transformation, we can "straighten" the board in the photo. Without this transformation step, if we would manually crop the board out of the image, we would see certain distortion (narrowing and shortening) in the parts of the board below camera level.

The key points (a total of 12), which are the corners of the coloured squares we painted, have their ideal positions precisely known. The task is therefore to find the corners of the squares (key points) in the real photos taken in the field. To do that, we run Shi-Tomasi corner detection (Shi and Tomasi, 1994) on the box images. Based on the coordinates of the detected key points, we can extract the orthophoto of the board from the original image using perspective transformation. Ideally, the resulting image fills the board (Fig. 2). However, in realistic cases, the bottom of the board is usually not matching accurately with the bottom of the image. In these cases the distance of bottom of the image and the 10 cm mark on the table deviates from the expected 10 cm which is the measurable error of the transformation.

2.4. Pixel analysis

The obtained orthophotos are suitable for pixel analysis. The sample area to be analyzed on the board is 99 × 31 (height x width) cm. The first step in pixel analysis is determining the average colour shade of the board, which is highly dependent on lighting conditions. This is done by cropping a 20 × 20 pixel square from the top right corner of the sample area (cropped whiteboard) and calculating the average, minimum, and maximum values for the three colour channels (R, G, B). By comparing the average values to the white colour code (255 on all three channels), we obtain information about the "whiteness" of the sample square (only in theory is the whiteboard completely white). If the board appears sufficiently white, we examine the differences between the maximum and minimum values for each colour channel. If this difference exceeds a certain threshold, it indicates that the pixels do not represent a uniform object (e.g., vegetation pixels protruding). If our sample square is not white enough or likely contains disturbances, we move left on the image and start analyzing another 20 × 20 pixel square until we find one that meets both criteria. Once we have found the appropriate sample square, its average values are treated as the average shade of the board. This is

Fig. 2. Reconstructed frontal orthophoto of the proposed whiteboard without vegetation. Each coloured square is 5 × 5 cm and the markings at the bottom have a gap of 1 cm. These markings help us to measure the error of the perspective transformation. (For interpretation of the references to colour in this figure legend, the reader is referred to the web version of this article.)

followed by the analysis of the entire sample area, where the our algorithm (git/web_app/scripts/veg_analyzer.py) "walks" through each pixel and categorizes it based on its colour code. Each pixel can be classified into two categories: either as part of the board or as vegetation. By saving the pixels along with their coordinates and assigned categories into a data table, we can calculate the four previously determined parameters (leaf area (LA), maximum height of vegetation (MHV), height of the closed vegetation (HCV), and foliage height diversity (FHD)). LA is the residue of vegetation pixels and all pixel multiplied by the product of board width (in cm) and board height (in cm). HCV is the largest height value where the vegetation pixels are greater than 0.95 in a pixel row. MHV is the largest height value where at least 1 vegation pixel is present in a pixel row. FHD is the shannon diversity of the number of vegetation pixels in each pixel row (Mizsei et al., 2024). Then the results are saved to a CSV file containing the image name and the corresponding calculated parameters.

2.5. *Quantifying transformation accuracy*

To quantify the error of perspective transformation, 120 test images were taken, divided into four categories. The basis of the categorization is determined by both the quality (resolution) of the images and the condition of the board. Some of the images were taken at a resolution of 3200 × 2400 (width x height, Olympus TG-4), while others were taken at a resolution of 6000 × 8000 (width x height, Xiaomi M2003j15SC). Regarding the condition of the board, we distinguish between the categories of "old" and "new". The back of the old board ends in a wide stake (in contrast to the new one, which has a nail attached to the bottom), resulting in less stability. Additionally, on the old board, the coloured squares were not drawn perfectly accurately; thin graphite lines were visible along the edges of the coloured squares. We resolved this by taping the borders and repainting the squares.

Based on all of this, there are four categories:

1. Old board, low-resolution images (30 images),
2. Old board, high-resolution images (30 images),
3. New board, low-resolution images (30 images),
4. New board, high-resolution images (30 images).

All test images were taken from a distance of 2 m (measured from the bottom of the board) and a height of 80 cm. Images of different resolution were taken under the same conditions (whiteboard location, whiteboard position), using different devices a few seconds apart. The results were verified based on the coordinates of the 10 cm markings shown at the bottom of the orthophotos (Fig. 2) on both sides. These images have a resolution of 1050 × 350 (height x width) pixels, so each centimetre, in reality, corresponds to 10 pixels in the image. The performance standard for the perspective transformation is when the bottom of the board perfectly aligns with the bottom of the image, so the 10 cm marking should be located at pixel position 950 on the Y-axis.

We manually recorded the real coordinates of the 10 cm markings in ImageJ software (Schneider et al., 2012) for the 120 images. We compared the ideal value (Y = 950) with the measured values. The difference between the real and the ideal value, divided by ten, gives the error in centimetres of the position of the board in the given image. Utilizing these error values, we characterized the method both individually for each category and as a whole. We determined the maximum (greatest positive deviation, where the bottom of the board is higher than the bottom of the image), minimum (greatest negative deviation, where the bottom of the board is lower than the bottom of the image), average error, and the distribution of errors.

We then investigated the effects of board renewal and resolution, using the R programming language (R Core Team, 2024). Since none of the error vectors followed a normal distribution, we used a two-sample Wilcoxon test ('wilcox.test' function in R) to compare the results of the two types of whiteboard. The error vectors of the different resolution

groups follow a normal distribution, but differ in variance, thus we used a two-sample Welch's *t*-test ('t.test' function in R) to compare the results.

2.6. Quantifying noise effect

The test images were captured in vegetation-free locations, allowing for the use of the centimetre-scale markings on the board for verification without any interference affecting the coloured squares. However, we wanted to test the effects of vertical, horizontal, and scattered disturbances on different reference squares and the consequences of covering an entire square.

We applied different types of noise layers on the NH images to simulate vegetation-like disturbance. We used GIMPs (The GIMP Development Team, 2024) built-in "Vegetation 02" brush for scattered noise and „Grass" brush for full square cover. We made custom brushes for horizontal and vertical noise, then applied them using GIMP (Fig. 3). We ran the scripts on the noisy images, then measured the coordinates of the 10 cm markings, like in the previous chapter. After that, we measured the effects of GIMP exportation itself (using non-modified NH results as control), and the effect of different noises, treating GIMP results as control. Four noise types (GIMP exportation, horizontal, vertical, and scattered noises) where the error vectors (noise and control) followed a normal distribution and didn't differ in variance, we used a two-sample Student's *t*-test ('t.test' function in R) to evaluate the effect. The error vectors of full square covered images differed in variance relative to the control, so we used a two-sample Welch's *t*-test ('t.test' function in R) to evaluate the effect.

2.7. Creating a user-executable web application

We have developed a user-executable web application to facilitate the use of the method, which can carry out the entire workflow for images. The application utilizes the power of Flask (Grinberg, 2014), a prominent web-development library for the Python programming language (van Rossum, 1995).

Using the application, there are two main ways to get the coordinates of key points, which are the foundation of perspective transformation: first is the manual recording using image processing software, and second is the automated detection proposed in this paper. Our application has a built-in annotator page, which allows the user to manually record, delete, and edit keypoint coordinates. This way of working requires more time and effort, but ensures more accurate transformations, thus we recommend using the annotator function only in the case of problematic, noisy images.

After running the automated image analysis using the web application, the user can review and edit the detected key points (key points are automatically drawn to the images, and the user can browse the images one by one). The user can then re-run the analysis, using the manually corrected, verified coordinates.

The output of the analysis is 3 files. The first is cut_coords.csv, which contains the coordinates of image cropping. The second is report.txt, which contains feedback about each process (results of object and keypoint detection, pixel analysis), listing the problematic images, making it easier for the user to filter errors. The third is vegetation_structure_results.csv, which contains the calculated structural parameters of each image. Documentation and code are available at: https://github.com/EvoZooDeb/whiteboard under the MIT licence.

3. Results

3.1. Object localization

The training of our model took 6 min and 41 s and inference takes 0.64 s/image on average (using a CPU, including cropping the "box images"). Our model evaluation results are summarized in Table 1. Both the validation and test dataset achieved a mAP50 score of 0.995, the precision on the validation set is 0.999 on the test set is 1.0, and the recall score on the validation set is 1.0 on the test set is 0.998. These metrics are almost perfect, so we can conclude that the object detection of our custom whiteboard is perfectly satisfactory.

3.2. Transformation

Running the transformation takes 0.898 s/image on average. The results of transformation accuracy are summarized in Table 2. Examining each of the categories in Table 2, the following results are clear:

- In the case of old board low resolution images, the transformation achieved an accuracy of 5 cm in 95 % of the images and an accuracy of 2.5 cm in 56.7 % of the images.
- In the case of old board high resolution images, the transformation achieved an accuracy of 5 cm in 83.3 % of the images and an accuracy of 2.5 cm in 56.7 % of the images.
- In the case of new board low resolution images, the transformation achieved an accuracy of 5 cm in 93.3 % of the images and an accuracy of 2.5 cm in 56.7 % of the images.
- In the case of new board high resolution images, the transformation achieved an accuracy of 5 cm in 100 % of the images and an accuracy of 2.5 cm in 76,6 % of the images.
- Examining the combined results in Table 2, we can see that the transformation achieved an accuracy of 5 cm in 92,9 % of the images and an accuracy of 2.5 cm in 61,6 % of the images.

The use of the new board resulted in significantly smaller transformation errors (p-value <0.0001) compared to old boards.

The transformation errors on high resolution images are significantly (p-value <0.005) smaller than the measured errors on low resolution images.

Table 1
Evaluation of our YOLOv8 object detection model: We used two different sets of images to evaluate our model's performance. The second column represents the Mean Average Precision (mAP) at the Intersection over Union (IoU) rate of 50.

Dataset	mAP50	Precision	Recall
Validation	0.995	0.999	1.0
Test	0.995	1.0	0.998

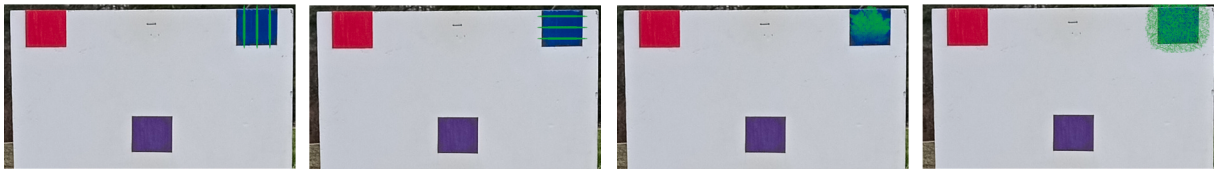

1. Vertical Noise **2. Horizontal Noise** **3. Scattered Noise** **4. Full Cover Noise**

Fig. 3. The different types of noise filters we used to simulate vegetation-like disturbances in the blue reference square. 1. Vertical Noise (custom brush), 2. Horizontal Noise (custom brush), 3. Scattered Noise ("Vegetation 02" brush from GIMP), 4. Full cover Noise ("Grass" brush from GIMP). (For interpretation of the references to colour in this figure legend, the reader is referred to the web version of this article.)

Table 2
Transformation evaluation. The first four rows contain the results for individual categories, and the fifth row represents the combined (C) results. The "Name" column indicates the board's condition (Old/New) and resolution (Low/High). The "Min," "Max," and "Mean" columns represent the errors in centimetres. The zones follow each other at intervals of 1.25 cm, so in Z_1, the percentage of images (rounded to the nearest whole number) where the absolute error is <1.25 cm is shown, and in the fifth zone, where the absolute error is >5 cm. The "NA" column represents the percentage of images where the 10 cm marking was not readable.

ID	Min	Max	Mean	Z_1	Z_2	Z_3	Z_4	Z_5	NA
OL	−2.92	6.05	1.29	21.7	35.0	21.7	16.7	3.3	1.7
OH	−2.05	6.6	2.28	16.7	40.0	20.0	6.7	10.0	6.7
NL	−5.68	4.25	−0.28	36.7	20.0	20.0	16.7	5.0	1.7
NH	−3.24	3.46	0.61	38.3	38.3	23.3	0	0	0
C	−5.68	6.6	0.96	28.3	33.3	21.2	10.0	4.6	2.5

3.3. Noise effects

The results of the noise effect on transformation accuracy are summarized in Table 3. The effect of GIMP exportation, vertical, horizontal, and scattered noise is not-significant (Table 3). The effect of covering a whole square is significant in the case of the red square (p-value <0.0001) and the purple square (p-value <0.0001). In the case of the blue square, the effect is not significant (Table 3).

4. Example application

4.1. Introduction

The Balkan Wall Lizard (*Podarcis tauricus*) is a widespread species in southeastern Europe, mainly in open, treeless, lowland areas. We lack knowledge of the biology, ecology and precise conservation status of this species in general, however, habitat loss, fragmentation and degradation can negatively impact and possibly reduce Balkan Wall Lizard populations (Mollov and Valkanova, 2009). The Balkan Wall Lizard can achieve high densities under ideal conditions, for instance, Mizsei et al., 2020 estimated 22,6 ± 1,56 individuals/ha (mean ± SE) in a sandy grassland in Central Hungary, which is the northwestern limit of the species distribution. The same study also showed that vegetation cover negatively affects the presence of the species, while abundance was positively connected with the presence of taller tussocks (Mizsei et al., 2020). As part of a current LIFE project (LIFE18 NAT/HU/000799), while monitoring the endangered Hungarian Meadow Viper populations in protected grasslands in Central Hungary, we also record the occurrence of other reptile species within the same habitats, such as the Balkan Wall Lizard. The monitoring indicates that the Balkan Wall Lizard is gradually disappearing from the area, highlighting the importance of identifying the factors that influence the lizards occurrence and habitat preference. Such knowledge is essential for optimising habitat management and ensuring the effective protection of these species. The density of the Balkan Wall Lizard presumably depends on different aspects of vegetation, therefore, we measured vegetation structural variables and examined their effect on the density of the species in the studied grassland complex.

4.2. Methods

Our study area included two large grassland areas in the Kiskunság National Park in Central Hungary, Felső-kiskunsági turjánvidék and Bócsa-bugaci homokpuszta (HUKN20003 and HUKN20024 Natura 2000 SCI sites). These grasslands represent a mosaic of diverse plant communities belonging to the priority habitat type Pannonian sand steppes (6260, EU Habitats Directive). The mosaic includes both primary and secondary grasslands, reflecting differences in land-use history, such as spontaneously regenerated abandoned fields and areas restored from former arable land. Here we designated and surveyed 99 semi-random sampling plots (seventy (50 × 50 m) and twenty-nine (100 × 100 m) plots). The sampling plots were surveyed 15 times, and a survey lasted at least 5 min, until the survey covered the whole plot area. The surveys were conducted between 7 AM and 7 PM, covering various weather conditions in the survey season, except heavy rain. We collected field data in the spring of 2024 between the 4th of April and the 25th of May. During the surveys, we recorded individually the observed Balkan Wall Lizards (coordinates, date, time, age and sex) using the OpenBioMaps android application (Bán et al., 2022). The operative temperature was recorded during the surveys using copper models to measure available environmental temperatures for a non-thermoregulating ectotherm individual (Kearney and Porter, 2020).

Vegetation structure was measured in the field by taking photographs against the whiteboard, as described in the materials and

Table 3
Noise effects on transformation accuracy. The first row contains the results of NH images. The second row contains the results of GIMP exported images. In the other rows, the "ID" column indicates the modified square (Red, Blue, Purple) and the noise type (Vertical, Horizontal, Scattered, Cover). The "Min," "Max," and "Mean" columns represent the errors in centimetres. The zones follow each other at intervals of 1.25 cm, so in Z_1, the percentage of images (rounded to the nearest whole number) where the absolute error is <1.25 cm is shown, and in the fifth zone, where the absolute error is >5 cm. The "NA" column represents the percentage of images where the 10 cm marking was not readable. The "p" column represents the rounded p-value of the used statistical test (Student's t-test for: control, gimp, rv, bv, pv, rh, bh, ph, rs, bs, ps. Welch's *t*-test for: rc, bc, pc).

ID	Min	Max	Mean	Z_1	Z_2	Z_3	Z_4	Z_5	NA	p
control	−3.24	3.46	0.61	38.3	38.3	23.3	0	0	0	–
gimp	−3.32	3.88	0.59	45.0	40.0	13.3	1.7	0	0	0.96
rv	−3.21	3.86	0.55	43.3	38.3	16.7	1.7	0	0	0.87
bv	−3.03	3.85	0.65	43.3	36.7	18.3	1.7	0	0	0.86
pv	−2.98	6.27	0.68	48.3	28.3	18.3	1.7	3.3	0	0.79
rh	−3.02	3.26	0.48	43.3	38.3	18	0	0	0	0.69
bh	−3.26	3.42	0.36	43.3	43.3	13.3	0	0	0	0.44
ph	−3.32	6.04	0.76	41.7	36.7	18.3	1.7	1.7	0	0.61
rs	−3.17	3.76	0.58	43.3	35.0	20.0	1.7	0	0	0.97
bs	−3.22	3.59	0.64	38.3	40.0	21.7	0	0	0	0.89
ps	−2.95	3.3	0.58	40.0	41.7	18.3	0	0	0	0.95
rc	−2.72	9.77	4.75	1.7	10.0	25.0	18.3	40.0	5.0	<0.0001
bc	−4.77	7.43	0.64	21.7	28.3	23.3	16.7	3.3	6.7	0.93
pc	−6.21	10.84	3.78	13.3	11.7	6.7	13.3	40.0	15.0	<0.0001

methods section. The whiteboard was placed in the vegetation on its shorter edge, and we took photos from 0,5 height and 4 m distance (Mizsei et al., 2024), in 25 locations, 10 m apart from each other, in every sampling plot between the 7th and 24th of May. The vegetation structure sampling resulted in 2475 photos available for analysis in total (25 photos for each 99 sites). Vegetation structure was quantified, and the variables (leaf area (LA), maximum height of vegetation (MHV), height of the closed vegetation (HCV), and foliage height diversity (FHD)) were calculated using the previously described methodology.

To assess the influence of vegetation structure on the density of the Balkan Wall Lizard, we used n-mixture models (Royle, 2004) fitted using the unmarked package in R (Fiske and Chandler, 2011). N-mixture models are widely used in ecological studies to estimate the abundance or density of organisms from count data while accounting for imperfect detection. These models simultaneously model the ecological process of interest (e.g., abundance) and the observation process (e.g., detection probability), making them particularly suitable for datasets with repeated observations at the same sites.

To identify vegetation structure variables influencing the lizards' density, we fitted a global model including all four variables and performed a model selection using the MuMIn package (Bartoń, 2018). In the model selection, we included the variable operative temperature and its quadratic term, which often influences the activity, thus the detectability of ectothermic species such as the Balkan Wall Lizard, while in the abundance (density) submodel, we iterated all combinations of the vegetation structure variables. The sampling plot area was a fixed offset in the models. To evaluate model candidates, we calculated Akaike's Information Criterion (AIC) to identify the most parsimonious model explaining the observed data (Akaike, 1998). The model candidates receiving a $\Delta AIC<2$ (ΔAIC = min(AIC)-AICi) were considered as best-fitting models (Burnham et al., 2004).

4.3. Results

During the total $n = 1485$ surveys conducted in the monitoring season, we detected $n = 297$ Balkan Wall Lizard individuals. The maximum number of observations per site was 15, while the mean number of observations per site was also 15. Out of the $n = 99$ sites, 39 sites had at least one detection. Among all surveys, we had 1328 surveys without a Balkan Wall Lizard detection, 95 with only 1 detection, and we were able to detect more than 1 individual in just 62 out of the total number of 1485 surveys.

The model selection retrieved a single model based on our selection criterion, including the variable temperature (and its quadratic term) in the detection submodel, and the density submodel three out of the four variables were included: HCV, LA, and MHV (Table S1). Temperature showed a significant non-linear influence on detectability (Table S2), while in the density submodels, leaf area (LA) had a significant negative effect, and maximum height of vegetation (MHV) and height of closed vegetation (HCV) significantly positively affected the density of the Balkan Wall Lizard (Table S3).

5. Discussion

Automated processing of field photographs presents a significant challenge due to the variability in environmental conditions, which can affect the quality of images. Nonetheless, in ecological research, there is an increasing need for automated methods to analyze vegetation structure, as they can greatly improve the speed, accuracy, and reliability of data processing. The method we have improved and developed addresses many of the limitations inherent in traditional field measurements – like the need of manual cropping and measurement of the vegetation, constraint to rely on unreproducible eye estimates - offering a reproducible, semi-automated solution to quantify key vertical parameters of vegetation. Our approach is effective in capturing important structural parameters like leaf area (LA), maximum height of vegetation (MHV), and height of closed vegetation (HCV), it proves to be both efficient and robust for characterizing vegetation structure across various habitats. Although our method tends to overestimate vegetation height, similar to others (e.g., Zehm et al., 2003). Using the proposed method, capturing an image takes approximately 2 min, while running the necessary scripts using the developed web-based application takes a few seconds per image.

Our case study on the Balkan Wall Lizard (*Podarcis tauricus*), a grassland specialist reptile, exemplifies the potential application of whiteboard photography to model the influence of vegetation on non-herbivorous animals. The results align well with previous studies that show the Balkan Wall Lizard prefers open grassland habitats with low vegetation cover (Mizsei et al., 2020; Vacheva and Naumov, 2024). In particular, the negative effect of leaf area (LA) on lizard density suggests that these reptiles avoid dense vegetation that limits their movement or visibility, consistent with their known preference for open spaces with better access to basking sites and easier navigation. Moreover, our findings indicate that vegetation complexity, as measured by MHV and HCV, positively influences lizard density, suggesting that structures like tussocks and other plant features may provide critical microhabitats and shelter, supporting higher densities in certain areas (Mizsei et al., 2020). This highlights the importance of vegetation complexity beyond the mere openness of the habitat in determining species density.

Despite these advancements, several limitations remain. First, the accuracy of the method can be influenced by perspective distortions, particularly when the whiteboard is not perfectly aligned or when the ground is uneven. Although we use a perspective transformation process to address this issue, slight inaccuracies may still occur, particularly in images with extreme distortion. Furthermore, lighting conditions, such as reflections from leaves or shadows cast on the whiteboard, can lead to misclassification of vegetation pixels. While adaptive thresholding helps mitigate this, the method may still struggle under challenging lighting conditions. Additionally, the accuracy of the method depends heavily on the quality of the photographs, and it is recommended to take images under consistent lighting conditions, ensuring the whiteboard is positioned straight and stable, with clearly visible square corners. It is also advisable to remove contaminants like mud from the board to maintain high image quality. In addition, placing the whiteboard on the ground in areas with dense vegetation during fieldwork can be challenging. As this method is primarily designed for grasslands and other open terrestrial habitats, the limited size of the board makes it less suitable for representing wooded or forested communities.

While the object detection model improves efficiency, it may not perform equally well across all vegetation types or habitats without further tuning (the problem of generalization). Unlike the training of most deep learning-based object detection algorithms, which require large and well-annotated datasets, our whiteboard detector performed optimally with a relatively small training set. Less demanding annotation efforts make training new models easier, which facilitates the customizability and adaptability of the method.

Additionally, the inherent inaccuracies in corner detection could impact the precision of the transformation. Comparing results using different corner detection algorithms may further refine the method's accuracy. The painting accuracy of the coloured squares used on the whiteboard has a significant effect on the calculation of the board distortion, therefore we recommend using printed stickers for better results. In our study, covering the red or purple squares in the image decreased the reliability of the method, while the blue square showed less impact on accuracy, warranting further investigation to understand these discrepancies.

Despite these limitations, the method offers substantial improvements over traditional field-based measurements and provides a flexible, scalable solution for quantifying vegetation structure. The photography-based approach eliminates the biases and errors coming from the manual estimation of human observers (Bergstedt et al., 2009; Milberg et al., 2008). Our methods accuracy for the vertical parameters is well

within the error range (5 cm) used for manual measurements (Lengyel et al., 2016), while being more reproducible and documented. However, using LiDAR/UAV techniques might yield more accurate measurements, but the required equipment and postprocessing skills serve as a bottleneck for the wider audience.

The user-friendly web application facilitates quick and reproducible measurements, making it a valuable tool for large-scale ecological studies and long-term monitoring. Further development of this method could expand its applicability, particularly in large-scale studies examining the distribution of various taxa, where it could offer valuable insights into habitat selection. Additionally, incorporating other parameters measured by the software described by Zehm et al. (2003) could further enhance the method's capabilities. If case studies confirm that the vegetation parameters derived through this method are indicative of habitat suitability for multiple taxa, it may be worthwhile to develop a mobile application for field use, allowing researchers to conduct real-time assessments in the field.

Supplementary data to this article can be found online at https://doi.org/10.1016/j.ecoinf.2025.103540.

CRediT authorship contribution statement

Gergő Oláh: Writing – original draft, Visualization, Software, Methodology. **Mátyás Budai:** Writing – review & editing, Investigation, Formal analysis. **Edvárd Mizsei:** Writing – review & editing, Methodology, Formal analysis. **Miklós Bán:** Writing – review & editing, Methodology.

Declaration of generative AI and AI-assisted technologies in the writing process

During the preparation of this work, the author(s) used Grammarly to enhance the clarity, grammar, and overall readability of the text, and ChatGPT to assist in removing repetitive parts and improving the flow of the text. After using these tools, the author(s) reviewed and edited the content as needed and take(s) full responsibility for the content of the publication.

Funding

Supported by the EKÖP-24-3 University Research Scholarship Program of the Ministry for Culture and Innovation from the source of the National Research, Development and Innovation Fund.

Data collection was implemented within the frames of the HUNVIPHAB 'Viability improvement of Hungarian meadow viper populations and habitats in the Pannonian region' (LIFE18 NAT/ HU/000799) LIFE project financed by the European Commission and the Hungarian Ministry of Agriculture.

Declaration of competing interest

The authors declare that they have no known competing financial interests or personal relationships that could have appeared to influence the work reported in this paper.

Acknowledgements

We are thankful for Csongor Adorjáni, Barnabás Bancsik, Zsombor Bányi, Gergő Kovács, Zsolt Ladnyik, Attila Móré, Bence Nagy, Dávid Radovics, Gergő Rák, Márton Szabolcs, Zsolt Villás, Bálint Wenner for their help in the Balkan Wall Lizard data collection.

This work benefited from services and resources provided by the EGI e-Infrastructure, with the dedicated support of ELKH-CLOUD.

Data availability

Code, measurements, models, documentation, and statistical analysis available at: https://github.com/EvoZooDeb/whiteboard/tree/main

Images and annotations are available at: https://vocs.unideb.hu/nextcloud/index.php/s/KazkcPKbbDdAzmC

References

Akaike, H., 1998. Information theory and an extension of the maximum likelihood principle. In: Springer Series in Statistics, pp. 199–213. https://doi.org/10.1007/978-1-4612-1694-0_15.

Bán, Miklós, Boné, Gábor Máté, Bérces, Sándor, Barta, Zoltán, Kovács, István, Ecsedi, Kornél, Sipos, Katalin, 2022. OpenBioMaps – self-hosted data management platform and distributed service for biodiversity related data. Earth Sci. Inf. 15 (3), 2007–2016. https://doi.org/10.1007/s12145-022-00818-3.

Bartoń, K., 2018. MuMIn: Multi-Model Inference (1.47.5).

Benkobi, Lakhdar, Uresk, Daniel W., Schenbeck, Greg, King, Rudy M., 2000. Protocol for monitoring standing crop in grasslands using visual obstruction. J. Range Manage. 53 (6), 627. https://doi.org/10.2307/4003158.

Bergstedt, Johan, Westerberg, Lars, Milberg, Per, 2009. In the eye of the beholder: bias and stochastic variation in cover estimates. Plant Ecol. 204 (2), 271–283. https://doi.org/10.1007/s11258-009-9590-7.

Boulinier, Thierry, Nichols, James D., Sauer, John R., Hines, James E., Pollock, K.H., 1998. Estimating species richness: the importance of heterogeneity in species detectability. Ecology 79 (3), 1018–1028. https://doi.org/10.1890/0012965819980079[1018:ESRTIO]2.0.CO;2.

Bradski, G., 2000. The OpenCV library. In: *Dr.* Dobb's Journal of Software Tools, 120, pp. 122–125.

Burnham, K., Anderson, D., Calvin, J., Burnham, S., Anderson, L., Anderson, D., Anderson, A., Akaike, H., Leibler, R., Shibata, R., Takeuchi, K., Anderson, D., 2004. Model selection and multimodel inference. In: Springer eBooks. https://doi.org/10.1007/b97636.

Cody, M.L., 1981. Habitat selection in birds: the roles of vegetation structure, competitors, and productivity. BioScience 31 (2), 107–113. https://doi.org/10.2307/1308252.

CVAT.Ai Corporation, 2023. Computer Vision Annotation Tool (CVAT).

Easlon, Hsien Ming, Bloom, Arnold J., 2014. Easy leaf area: automated digital image analysis for rapid and accurate measurement of leaf area. Appl. Plant Sci. 2 (7), 1400033. https://doi.org/10.3732/apps.1400033.

Fiske, Ian, Chandler, Richard, 2011. Unmarked: an R package for fitting hierarchical models of wildlife occurrence and abundance. J. Stat. Softw. 43 (10). https://doi.org/10.18637/jss.v043.i10.

Garden, Jenni G., Mcalpine, Clive A., Possingham, Hugh P., Jones, Darryl N., 2007. Habitat structure is more important than vegetation composition for local-level management of native terrestrial reptile and small mammal species living in urban remnants: a case study from Brisbane, Australia. Austral Ecol. 32 (6), 669–685. https://doi.org/10.1111/j.1442-9993.2007.01750.x.

Grinberg, Miguel, 2014. Flask Web Development, First edition. O'Reilly, Sebastopol, CA.

Jocher, G., Chaurasia, A., Qiu, J., 2023. YOLO by Ultralytics. https://github.com/ultralytics/ultralytics.

Kearney, Michael R., Porter, Warren P., 2020. NicheMapR – an R package for biophysical modelling: the ectotherm and dynamic energy budget models. Ecography 43 (1), 85–96. https://doi.org/10.1111/ecog.04680.

Kreft, Holger, Jetz, Walter, 2007. Global patterns and determinants of vascular plant diversity. Proc. Natl. Acad. Sci. 104 (14), 5925–5930. https://doi.org/10.1073/pnas.0608361104.

Lawton, J.H., 1983. Plant architecture and the diversity of phytophagous insects. Annu. Rev. Entomol. 28 (1), 23–39. https://doi.org/10.1146/annurev.en.28.010183.000323.

Lengyel, Szabolcs, Déri, Eszter, Magura, Tibor, 2016. Species richness responses to structural or compositional habitat diversity between and within grassland patches: a multi-taxon approach. edited by B. Boldgiv PLoS One 11 (2), e0149662. https://doi.org/10.1371/journal.pone.0149662.

Lin, Tsung-Yi, Maire, Michael, Belongie, Serge, Bourdev, Lubomir, Girshick, Ross, Hays, James, Perona, Pietro, Ramanan, Deva, Zitnick, C. Lawrence, Dollár, Piotr, 2014. Microsoft COCO: Common Objects in Context.

Loke, Lynette H.L., Ladle, Richard J., Bouma, Tjeerd J., Todd, Peter A., 2015. Creating complex habitats for restoration and reconciliation. Ecol. Eng. 77, 307–313. https://doi.org/10.1016/j.ecoleng.2015.01.037.

McCoy, E.D., Bell, S.S., 1991. Habitat structure: the evolution and diversification of a complex topic. In: Bell, Susan S., McCoy, Earl D., Mushinsky, H.R. (Eds.), Habitat Structure. Springer Netherlands, Dordrecht, pp. 3–27.

Milberg, Per, Bergstedt, Johan, Fridman, Jonas, Odell, Gunnar, Westerberg, Lars, 2008. Observer bias and random variation in vegetation monitoring data. J. Veg. Sci. 19 (5), 633–644. https://doi.org/10.3170/2008-8-18423.

Mizsei, Edvárd, Fejes, Zsófia, Malatinszky, Ákos, Lengyel, Szabolcs, Vadász, Csaba, 2020. Reptile responses to vegetation structure in a grassland restored for an endangered snake. Community Ecol. 21 (2), 203–212. https://doi.org/10.1007/s42974-020-00019-2.

Mizsei, E., Budai, M., Rák, G., Bancsik, B., Radovics, D., Szabolcs, M., Móré, A., Vadász, C., Dudás, G., Lengyel, S., 2024. Microhabitat selection of meadow and steppe vipers enlightened by digital photography and image processing to describe grassland vegetation structure. J. Zool. 322 (2), 168–178. https://doi.org/10.1111/jzo.13129.

Mollov, I.A., Valkanova, M.V., 2009. Risks and opportunities of urbanization – structure of two populations of the Balkan Wall lizard Podarcis tauricus (Pallas, 1814) in the City of Plovdiv. Ecol. Balkanica 1, 27–39.

Novotny, Vojtech, Drozd, Pavel, Miller, Scott E., Kulfan, Miroslav, Janda, Milan, Basset, Yves, Weiblen, George D., 2006. Why are there so many species of herbivorous insects in tropical rainforests? Science 313 (5790), 1115–1118. https://doi.org/10.1126/science.1129237.

R Core Team, 2024. R: A Language and Environment for Statistical Computing. R Foundation for Statistical Computing. https://www.R-project.org/.

Robel, R.J., Briggs, J.N., Dayton, A.D., Hulbert, L.C., 1970. Relationships between visual obstruction measurements and weight of grassland vegetation. J. Range Manage. 23 (4), 295. https://doi.org/10.2307/3896225.

Royle, J. Andrew, 2004. N -mixture models for estimating population size from spatially replicated counts. Biometrics 60 (1), 108–115. https://doi.org/10.1111/j.0006-341X.2004.00142.x.

Schneider, Caroline A., Rasband, Wayne S., Eliceiri, Kevin W., 2012. NIH image to ImageJ: 25 years of image analysis. Nat. Methods 9 (7), 671–675. https://doi.org/10.1038/nmeth.2089.

Shi, Jianbo, Tomasi, 1994. Good features to track. In: *Proceedings of IEEE Conference on Computer Vision and Pattern Recognition* CVPR-94. IEEE Comput. Soc. Press, Seattle, WA, USA, pp. 593–600.

Stein, Anke, Kreft, Holger, 2015. Terminology and quantification of environmental heterogeneity in species-richness research: environmental heterogeneity and species richness. Biol. Rev. 90 (3), 815–836. https://doi.org/10.1111/brv.12135.

Stein, Anke, Gerstner, Katharina, Kreft, Holger, 2014. Environmental heterogeneity as a universal driver of species richness across taxa, biomes and spatial scales. edited by H. Arita Ecol. Lett. 17 (7), 866–880. https://doi.org/10.1111/ele.12277.

Tews, J., Brose, U., Grimm, V., Tielbörger, K., Wichmann, M.C., Schwager, M., Jeltsch, F., 2004. Animal species diversity driven by habitat heterogeneity/diversity: the importance of keystone structures: animal species diversity driven by habitat heterogeneity. J. Biogeogr. 31 (1), 79–92. https://doi.org/10.1046/j.0305-0270.2003.00994.x.

The GIMP Development Team, 2024. GNU Image Manipulation Program (GIMP), Version 3.0.2. https://gimp.org.

Uetz, G.W., 1991. Habitat structure and spider foraging. In: Bell, S.S., McCoy, E.D., Mushinsky, H.R. (Eds.), Habitat Structure. Springer Netherlands, Dordrecht, pp. 325–348.

Vacheva, E., Naumov, B., 2024. Some insights into the diet of the Balkan wall lizard *Podarcis tauricus* (Pallas, 1814) in northwestern Bulgaria. Biharean Biol. 18 (1), 51–56.

van Rossum, G., 1995. Python Software Foundation. Python Language Reference, Version : 3.8.11. http://www.python.org.

Vermeire, Lance T., Gillen, Robert L., 2001. Estimating herbage standing crop with visual obstruction in tallgrass prairie. J. Range Manage. 54 (1), 57. https://doi.org/10.2307/4003528.

Zehm, Andreas, Nobis, Michael, Schwabe, Angelika, 2003. Multiparameter analysis of vertical vegetation structure based on digital image processing. Flora 198 (2), 142–160. https://doi.org/10.1078/0367-2530-00086.